

# An Overview of Signal Processing Techniques for RIS-aided Wireless Systems

Cunhua Pan

National Mobile Communications Research Lab.  
Southeast University

12<sup>th</sup> Aug. 2022

# Outline

- ① Research Background
- ② Cascaded Channel Estimation
- ③ Transmission Design
- ④ RIS-aided Localization/Sensing
- ⑤ Future Research Directions
- ⑥ Conclusion

# Related Paper

This article has been accepted for publication in IEEE Journal of Selected Topics in Signal Processing. This is the author's version which has not been fully edited and content may change prior to final publication. Citation information: DOI 10.1109/JSTSP.2022.3195671

1

## An Overview of Signal Processing Techniques for RIS/IRS-aided Wireless Systems

Cunhua Pan, Gui Zhou, Kangda Zhi, Sheng Hong, Tuo Wu, Yijin Pan, Hong Ren, Marco Di Renzo, *Fellow, IEEE*, A. Lee Swindlehurst, *Fellow, IEEE*, Rui Zhang, *Fellow, IEEE*, and Angela Yingjun Zhang, *Fellow, IEEE*

**Abstract**—In the past as well as present wireless communication systems, the wireless propagation environment is regarded as an uncontrollable black box that impairs the received signal quality, and its negative impacts are compensated for by relying on the design of various sophisticated transmission/reception schemes. However, the improvements through applying such schemes operating at two endpoints (i.e., transmitter and receiver) only are limited even after five generations of wireless systems. Reconfigurable intelligent surface (RIS) or intelligent reflecting surface (IRS) have emerged as a new and promising technology that can configure the wireless environment in a favorable manner by properly tuning the phase shifts of a large number of quasi passive and low-cost reflecting elements, thus standing out as a promising candidate technology for the next-sixth-generation (6G) wireless system. However, to reap the performance benefits promised by RIS/IRS, efficient signal processing techniques are crucial, for a variety of purposes such as channel estimation, transmission design, radio localization, and so on. In this paper, we provide a comprehensive overview of recent advances on RIS/IRS-aided wireless systems from the signal processing perspective. We also highlight promising research directions that are worthy of investigation in the future.

### I. INTRODUCTION

While the fifth-generation (5G) of wireless communication systems is under deployment worldwide, research interest has shifted to the future sixth-generation (6G) of wireless systems [1]–[3], which targets supporting not only cutting-edge applications like multisensor augmented/virtual reality applications, wireless brain computer interactions, and fully autonomous systems, but also the wireless evolution from “connected things” to “connected intelligence”. The required key performance indicators (KPIs), including data rates, reliability, latency, spectrum/energy efficiency, and connection density, will be superior to those for 5G. For example, the energy and spectrum efficiency for 6G are expected to be 10–100 times and 5 times better than those of 5G, respectively. These KPIs, however, cannot be fully achieved by the existing three-pillar 5G physical layer techniques [4], which include massive multiple-input multiple-output (MIMO), millimeter wave (mmWave) communications, and ultra-dense heterogeneous networks. In particular a large number

C. Pan et al., “An Overview of Signal Processing Techniques for RIS/IRS-aided Wireless Systems,” early access in IEEE Journal of Selected Topics in Signal Processing, 2022, doi: 10.1109/JSTSP.2022.3195671.



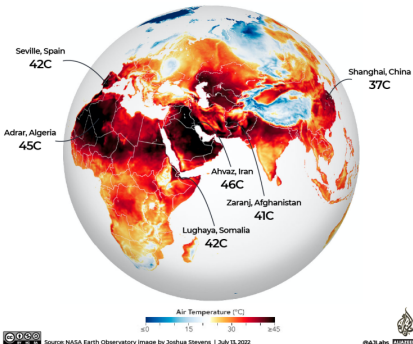
# Research Background

# Global Warming

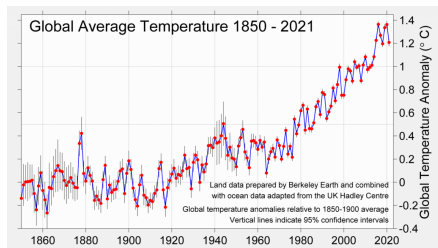
## WEATHER

### Heatwaves around the world

Extreme heat has struck Europe, North Africa, the Middle East and Asia, as temperatures climbed above 40C (104F) in many places fuelling wildfires and causing heat-related deaths.



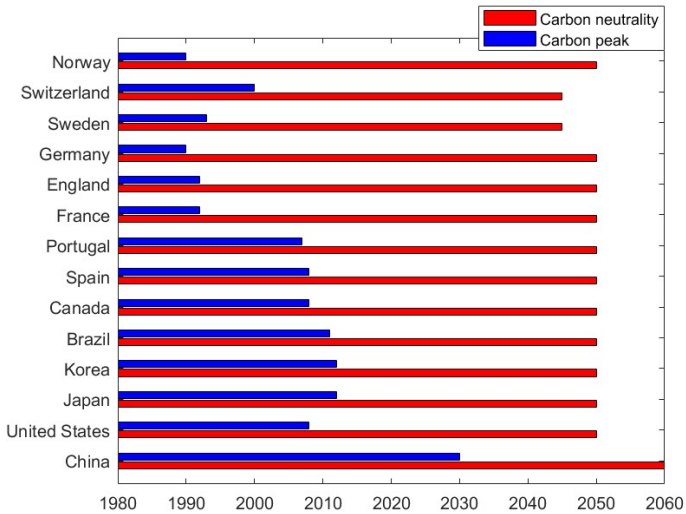
Source: NASA Earth Observatory image by Joshua Stevens | July 13, 2022



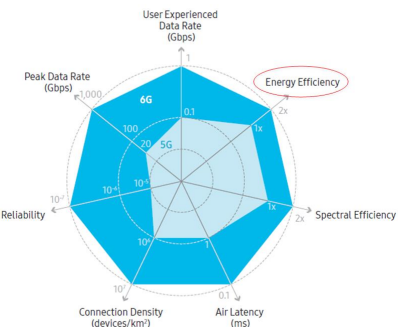
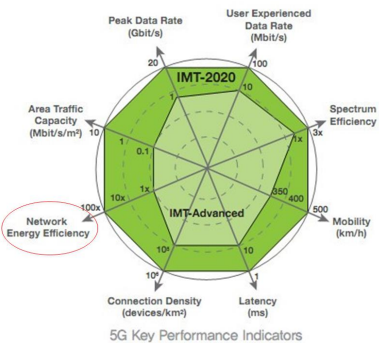
The temperature **increases rapidly** in the recent 50 years.

**Outcomes:** Glacial fusion, sea level rise, increase of diseases and pests, adverse weather, desertification area increases, etc

# Carbon Peaking and Carbon Neutrality Goals



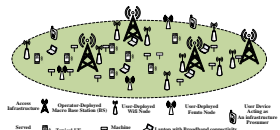
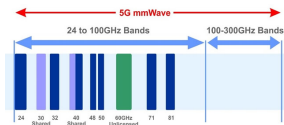
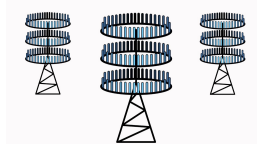
# Energy Efficiency Goals in 5G and 6G



Compared with LTE-Advanced, EE in 5G should be improved by **100 times**.

Compared with 5G, EE in 6G should be improved by **2 times**.

# Revisit Three Pillar Techniques in 5G



- ① Large number of RF chains
- ② High hardware cost
- ③ Difficult deployment
- ① High-frequency RF chains
- ② Readily to be blocked
- ③ High hardware cost

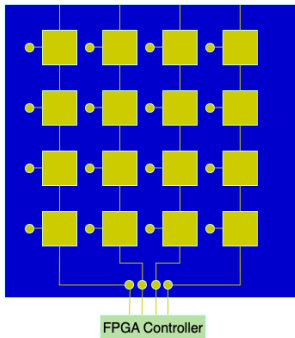
- ① Large number of BSs
- ② Complicated multi-BS interference mitigation techniques
- ③ High hardware cost

## Any New Techniques?

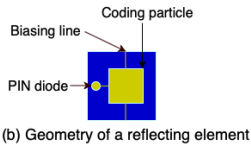
J. G. Andrews et al., "What Will 5G Be?," in IEEE Journal on Selected Areas in Communications, vol. 32, no. 6, pp.

1065-1082, June 2014

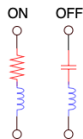
# Reconfigurable Intelligent Surfaces (RIS)



(a) Schematic of a configurable meta-surface prototype



(b) Geometry of a reflecting element



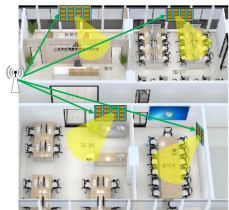
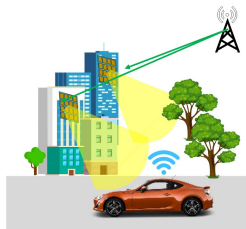
- ① Each reflection element includes one or more PIN diodes
- ② Reflection coefficients by varying the operating status of PIN diodes
- ③ Discrete reflection coefficient is controlled by the FPGA controller

# Comparison with Relay

Table 1: **RIS vs. Relay**

	<b>RIS</b>	<b>AF Relay</b>	<b>DF Relay</b>	<b>Full-duplex Relay</b>
With RF Chains?	No	Yes	Yes	Yes
SP Capability?	No	No	Yes	Yes
Noise?	No	Yes	Yes	Yes
Duplex	Full	Half	Half	Full
Hardware cost	Low	Median	High	Very high
Power Consumption	Low	Median	High	Very high

# User Cases for RIS (Easy Deployment)



# System Model in RIS-aided Communications Systems

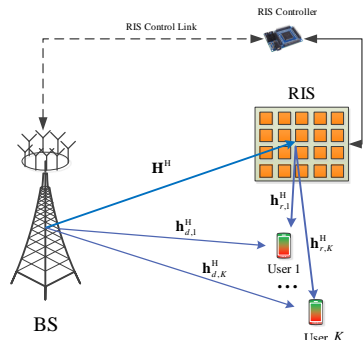


Figure 1: A multiple-antenna RIS-aided downlink system.

Then, the received signal can be rewritten as

$$y_k = (\mathbf{h}_{d,k}^H + \mathbf{G}_k^H \boldsymbol{\theta}) \sum_{j=1}^K \mathbf{w}_j s_j + n_k.$$

Received signal at user  $k$  is expressed as

$$y_k = (\mathbf{h}_{d,k}^H + \mathbf{h}_{r,k}^H \boldsymbol{\Theta} \mathbf{H}^H) \sum_{j=1}^K \mathbf{w}_j s_j + n_k,$$

where  $\mathbf{w}_k$  is the beamforming vector for user  $k$ ,  $\boldsymbol{\Theta}$  is the phase shift matrix at the RIS given by  $\boldsymbol{\Theta} = \text{diag}(\boldsymbol{\theta})$ ,  $\boldsymbol{\theta} = [\theta_1, \dots, \theta_M]^T$  with  $\theta_m = e^{j\varphi_m}$ .

Denote the **cascaded channel** for user  $k$  as  $\mathbf{G}_k^H \triangleq \text{diag}(\mathbf{h}_{r,k}^H) \mathbf{H}^H$ .

# Cascaded Channel Estimation

# Uplink Pilot Signal Transmission Model

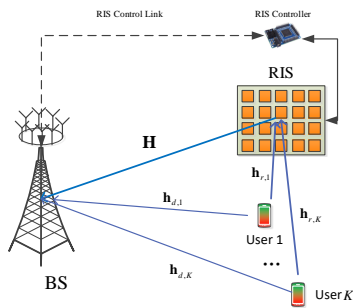


Figure 2: An RIS-aided uplink communication system

Then, the received signal can be rewritten as

$$\mathbf{y}_t = \sum_{k=1}^K \sqrt{P_k} (\mathbf{h}_{d,k} + \mathbf{G}_k \boldsymbol{\theta}_t) x_{k,t} + \mathbf{n}_t. \quad (1)$$

At time slot  $t$ , the received baseband signal at the BS is given by

$$\mathbf{y}_t = \sum_{k=1}^K \sqrt{P_k} (\mathbf{h}_{d,k} + \mathbf{H} \boldsymbol{\Theta}_t \mathbf{h}_{r,k}) x_{k,t} + \mathbf{n}_t,$$

where  $\boldsymbol{\Theta}_t$  is the phase shift matrix at the RIS, given by  $\boldsymbol{\Theta}_t = \text{diag}(\boldsymbol{\theta}_t)$ , and  $\boldsymbol{\theta}_t = [\theta_{t,1}, \dots, \theta_{t,M}]^T$  with  $\theta_{t,m} = e^{j\varphi_{t,m}}$ . Denote the cascaded channel for user  $k$  as  $\mathbf{G}_k = \mathbf{H} \text{diag}(\mathbf{h}_{r,k}) \in \mathbb{C}^{N \times M}$ .

## Unstructured Channel Models (Sub-6 GHz)

## Single-user Case

The received signal model at time slot  $t$  becomes

$$\mathbf{y}_t = \sqrt{P}(\mathbf{h}_d + \mathbf{G}\boldsymbol{\theta}_t)x_t + \mathbf{n}_t. \quad (2)$$

The  $m$ -th column of  $\mathbf{G}$  is denoted by  $\mathbf{g}_m$ . Define  $\mathbf{H} = [\mathbf{h}_1, \dots, \mathbf{h}_M]$  and  $\mathbf{h}_r = [h_r^1; \dots; h_r^M]$ . Then,  $\mathbf{g}_m = h_r^m \mathbf{h}_m$ . By defining the overall channel as  $\mathbf{c} = [\mathbf{h}_d^T, \mathbf{g}_1^T, \dots, \mathbf{g}_M^T]^T$ , (2) can be rewritten as

$$\mathbf{y}_t = \sqrt{P} (x_t [1, \boldsymbol{\theta}_t^T] \otimes \mathbf{I}_N) \mathbf{c} + \mathbf{n}_t. \quad (3)$$

Assume that  $T$  time slots are used for channel training, i.e.,  $T$  time slots are reserved for estimating the end-to-end channel, and define

$$\boldsymbol{\Phi} = \begin{bmatrix} 1, \boldsymbol{\theta}_1^T \\ \dots \\ 1, \boldsymbol{\theta}_T^T \end{bmatrix} \in \mathbb{C}^{T \times (M+1)}, \boldsymbol{\Xi} = \boldsymbol{\Phi} \otimes \mathbf{I}_N. \quad (4)$$

## Single-user Case

Stacking the  $T$  training time slots together, the overall received signal vector can be expressed as

$$\begin{bmatrix} \mathbf{y}_1 \\ \vdots \\ \mathbf{y}_T \end{bmatrix} = \sqrt{P} \begin{bmatrix} x_1 [1, \boldsymbol{\theta}_1^T] \otimes \mathbf{I}_N \\ \vdots \\ x_T [1, \boldsymbol{\theta}_T^T] \otimes \mathbf{I}_N \end{bmatrix} \mathbf{c} + \begin{bmatrix} \mathbf{n}_1 \\ \vdots \\ \mathbf{n}_T \end{bmatrix}$$

$$= \sqrt{P} \mathbf{X} \boldsymbol{\Xi} \mathbf{c} + \mathbf{n}, \quad (5)$$

where we have defined  $\mathbf{X} = \text{diag}([x_1 \mathbf{1}_N; \dots; x_T \mathbf{1}_N])$  and  $\mathbf{n} = [\mathbf{n}_1^T, \dots, \mathbf{n}_T^T]^T$ . By defining  $\mathbf{y} = [\mathbf{y}_1^T, \dots, \mathbf{y}_T^T]^T$  and  $\mathbf{Z} = \mathbf{X} \boldsymbol{\Xi}$ , the received signal vector in (2) can be written as

$$\mathbf{y} = \sqrt{P} \mathbf{Z} \mathbf{c} + \mathbf{n}. \quad (6)$$

# Method I: Least Squares (LS) Estimator

The simplest method to estimate  $\mathbf{c}$  is the LS estimator, which is formulated as

$$\hat{\mathbf{c}} = \arg \min_{\mathbf{c}} \left\| \mathbf{y} - \sqrt{P} \mathbf{Z} \mathbf{c} \right\|^2, \quad (7)$$

for which the solution is

$$\hat{\mathbf{c}} = \frac{1}{\sqrt{P}} (\mathbf{Z}^H \mathbf{Z})^{-1} \mathbf{Z}^H \mathbf{y}. \quad (8)$$

The error covariance matrix of the estimated channel is:

$$\begin{aligned} \mathbf{R}_e &= \mathbb{E} \left\{ (\mathbf{c} - \hat{\mathbf{c}}) (\mathbf{c} - \hat{\mathbf{c}})^H \right\} \\ &= \frac{1}{P} \mathbb{E} \left\{ (\mathbf{Z}^H \mathbf{Z})^{-1} \mathbf{Z}^H \mathbf{n} \mathbf{n}^H \mathbf{Z} (\mathbf{Z}^H \mathbf{Z})^{-1} \right\} \\ &= \frac{\sigma^2}{P} (\mathbf{Z}^H \mathbf{Z})^{-1} = \frac{\sigma^2}{P} (\boldsymbol{\Xi}^H \boldsymbol{\Xi})^{-1} = \frac{\sigma^2}{P} (\boldsymbol{\Phi}^H \boldsymbol{\Phi})^{-1} \otimes \mathbf{I}_N. \end{aligned} \quad (9)$$

# Method I: Least Squares (LS) Estimator

On-off Scheme:

The training phase shift matrix is given by

$$\Phi = \begin{bmatrix} 1 & \mathbf{0}_M^T \\ \mathbf{1}_M & \mathbf{I}_M \end{bmatrix}. \quad (10)$$

DFT Scheme:

The training phase shift matrix  $\Phi$  is equal to the first  $M + 1$  columns of a  $T \times T$  DFT matrix, which is given by

$$[\Phi]_{t,m} = e^{-j \frac{2\pi(t-1)(m-1)}{T}}, t = 1, \dots, T, m = 1, \dots, M + 1.$$

Hadamard Matrix:

The training phase shift matrix can also be designed using the first  $M + 1$  columns of a  $T \times T$  Hadamard matrix, where  $T = 2^n, n = 1, 2, \dots$

## Method II: Linear Minimum Mean-Squared-Error (LMMSE)

The three channels in the RIS-aided system model can be written as

$$\mathbf{H} = \mathbf{R}_{\text{HB}}^{\frac{1}{2}} \tilde{\mathbf{H}} \mathbf{R}_{\text{HR}}^{\frac{1}{2}}, \mathbf{h}_r = \mathbf{R}_{\text{h}_r \text{R}}^{\frac{1}{2}} \tilde{\mathbf{h}}_r, \mathbf{h}_d = \mathbf{R}_{\text{h}_d \text{B}}^{\frac{1}{2}} \tilde{\mathbf{h}}_d, \quad (11)$$

where  $\mathbf{R}_{\text{HB}}$ ,  $\mathbf{R}_{\text{h}_d \text{B}}$ ,  $\mathbf{R}_{\text{h}_r \text{R}}$  and  $\mathbf{R}_{\text{HR}}$  are the spatial correlation matrices. The LMMSE of  $\mathbf{c}$  is given by

$$\hat{\mathbf{c}} = \mathbb{E}[\mathbf{c}] + \sqrt{P} \mathbf{C}_{\mathbf{cc}} \mathbf{Z}^H (P \mathbf{Z} \mathbf{C}_{\mathbf{cc}} \mathbf{Z}^H + \sigma^2 \mathbf{I}_{TN})^{-1} (\mathbf{y} - \bar{\mathbf{y}}), \quad (12)$$

where  $\mathbf{C}_{\mathbf{cc}} = \mathbb{E}[\mathbf{cc}^H]$  and  $\bar{\mathbf{y}} = \mathbb{E}\{\mathbf{y}\}$ . The matrix  $\mathbf{C}_{\mathbf{cc}}$  can be formulated as

$$\mathbf{C}_{\mathbf{cc}} = \begin{bmatrix} \mathbf{R}_{\text{h}_d \text{B}} & \mathbf{0}_{N \times MN} \\ \mathbf{0}_{MN \times N} & (\mathbf{R}_{\text{h}_r \text{R}} \odot \mathbf{R}_{\text{HR}}) \otimes \mathbf{R}_{\text{HB}} \end{bmatrix}. \quad (13)$$

## Reduced Pilot Overhead Scheme

Pilot overhead for the LS or the LMMSE estimators are  $T \geq (M + 1)$ .

## Element Grouping (EG) Method:

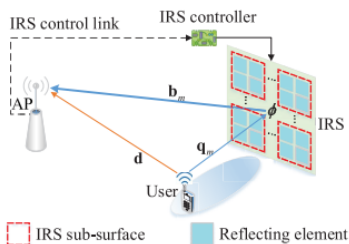


**Figure 3:** An illustration of EG method

- ① EG method groups the adjacent elements and assigns the same reflection pattern to them
  - ② Assume that the group size is  $J$ , the number of groups is  $M' = M/J$
  - ③ Minimum training pilot overhead is  $M' + 1$

# Simulation Results

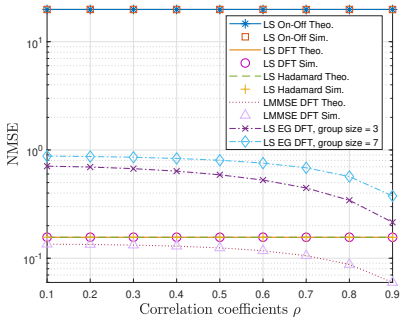


Figure 4: NMSE comparison of different channel estimation schemes.

- ① LS-on-off scheme has the worst NMSE
- ② LMMSE DFT approach offers the best estimation accuracy
- ③ The NMSE of the LS EG DFT method decreases by increasing the spatial correlation
- ④ The EG scheme is effective when the reflecting elements are strongly correlated

# Related References

- ① C. Pan et al., "An Overview of Signal Processing Techniques for RIS/IRS-aided Wireless Systems," in IEEE Journal of Selected Topics in Signal Processing, 2022
- ② Y. Yang, B. Zheng, S. Zhang, and R. Zhang, "Intelligent reflecting surface meets OFDM: Protocol design and rate maximization," IEEE Trans. Commun., vol. 68, no. 7, pp. 4522-4535, Jul. 2020
- ③ B. Zheng and R. Zhang, "Intelligent reflecting surface-enhanced OFD-M: Channel estimation and reflection optimization," IEEE Wireless Commun. Lett., vol. 9, no. 4, pp. 518-522, Jul. 2020.
- ④ T. L. Jensen and E. De Carvalho, "An optimal channel estimation scheme for intelligent reflecting surfaces based on a minimum variance unbiased estimator," in ICASSP 2020 - 2020 IEEE International Conference on Acoustics, Speech and Signal Processing (ICASSP), May 2020, pp. 5000-5004.
- ⑤ C. You, B. Zheng, and R. Zhang, "Channel estimation and passive beamforming for intelligent reflecting surface: Discrete phase shift and progressive refinement," IEEE J. Sel. Areas Commun., vol. 38, no. 11, pp. 2604-2620, Nov. 2020.
- ⑥ N. K. Kundu and M. R. McKay, "Channel estimation for reconfigurable intelligent surface aided MISO communications: From LMMSE to deep learning solutions," IEEE Open J. Commun. Soc., vol. 2, pp. 471-487, Mar. 2021.
- ⑦ A. L. Swindlehurst, G. Zhou, R. Liu, C. Pan and M. Li, "Channel Estimation With Reconfigurable Intelligent Surfaces—A General Framework," in Proceedings of the IEEE, 2022

# Cascaded Channel Estimation for Multiuser Scenarios

## Method I: Direct Channel Estimation Method

In the  $t$ -th sub-phase, the received training signal  $\mathbf{Y}_t \in \mathbb{C}^{N \times K}$  at the BS is given by

$$\mathbf{Y}_t = \sum_{k=1}^K \sqrt{P_k} (\mathbf{h}_{d,k} + \mathbf{G}_k \boldsymbol{\theta}_t) \mathbf{x}_k^T + \mathbf{N}_t, \quad t = 1, \dots, T, \quad (14)$$

where  $\mathbf{x}_k = [x_{k,1}, \dots, x_{k,K}]^T \in \mathbb{C}^{K \times 1}$ , such that  $\mathbf{x}_k^H \mathbf{x}_l = 0$  for  $k \neq l, \forall l, k$ , and  $\mathbf{x}_k^H \mathbf{x}_k = K$ .

By right multiplying both sides of (14) with  $\mathbf{x}_k^*$ , we have

$$\mathbf{y}_{t,k} = \sqrt{P_k} (\mathbf{h}_{d,k} + \mathbf{G}_k \boldsymbol{\theta}_t) + \mathbf{n}_{t,k}, \quad t = 1, \dots, T, \quad (15)$$

where  $\mathbf{y}_{t,k} = \mathbf{Y}_t \mathbf{x}_k^*$  and  $\mathbf{n}_{t,k} = \mathbf{N}_t \mathbf{x}_k^*$ .

For this scheme, the pilot overhead is equal to  $K(M + 1)$ .

# Cascaded Channel Estimation for Multiuser Scenarios

## Method II: Exploiting the Common RIS-BS Channel

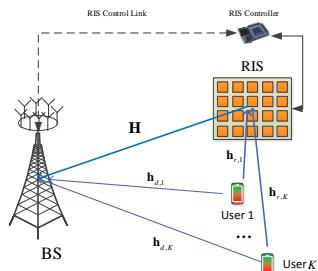


**Figure 5:** An RIS-aided uplink communication system

Pilot overhead:  $K + M + \max(K - 1, (K - 1) \lceil M/N \rceil)$ .

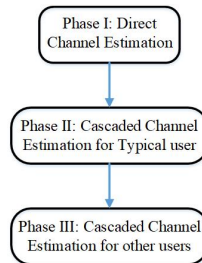


**Figure 6:** Three-phase cascaded channel estimation

Z. Wang, L. Liu, and S. Cui, "Channel estimation for intelligent reflecting surface assisted multiuser communications: Framework, algorithms, and analysis," IEEE Trans. Wireless Commun., vol. 19, no. 10, pp. 6607–C6620, Oct. 2020.

# Related References

- ① Q.-U.-A. Nadeem, H. Alwazani, A. Kammoun, A. Chaaban, M. Deb- bah, and M.-S. Alouini, "Intelligent reflecting surface-assisted multi- user MISO communication: Channel estimation and beamforming design," IEEE Open J. Commun. Soc., vol. 1, pp. 661 C680, May 2020.
- ② Z. Wang, L. Liu, and S. Cui, "Channel estimation for intelligent reflect- ing surface assisted multiuser communications: Framework, algorithms, and analysis," IEEE Trans. Wireless Commun., vol. 19, no. 10, pp. 6607 C6620, Oct. 2020.
- ③ B. Zheng, C. You, and R. Zhang, "Intelligent reflecting surface assisted multi-user OFDMA: Channel estimation and training design," IEEE Trans. Wireless Commun., vol. 19, no. 12, pp. 8315 C8329, Dec. 2020.
- ④ Y. Wei, M.-M. Zhao, M.-J. Zhao, and Y. Cai, "Channel estimation for IRS-aided multiuser communications with reduced error propagation," IEEE Trans. Wireless Commun., vol. 21, no. 4, pp. 2725 C2741, 2022.
- ⑤ H. Guo and V. K. N. Lau, "Uplink cascaded channel estimation for intelligent reflecting surface assisted multiuser MISO systems," IEEE Trans. Signal Process., pp. 1 C14, 2022.

# Structured Channel Models (mmWave Com.)

# Multiuser Case

**Assumptions:** 1. No direct channel between BS and RIS; 2. Both BS and RIS are equipped with ULA

Saleh-Valenzuela (SV) Channel Model :

$$\mathbf{H} = \sum_{l=1}^L \alpha_l \mathbf{a}_N(\psi_l) \mathbf{a}_M^H(\omega_l), \mathbf{h}_k = \sum_{j=1}^{J_k} \beta_{k,j} \mathbf{a}_M(\varphi_{k,j}), \forall k \in \mathcal{K},$$

where  $\omega_l = \frac{d_{\text{RIS}}}{\lambda_c} \cos(\theta_l)$ ,  $\psi_l = \frac{d_{\text{BS}}}{\lambda_c} \cos(\phi_l)$ , and  $\varphi_{k,j} = \frac{d_{\text{RIS}}}{\lambda_c} \cos(\vartheta_{k,j})$ ,  $\mathbf{a}_X(x) = [1, e^{-i2\pi x}, \dots, e^{-i2\pi(X-1)x}]^T$ , with  $X \in \{M, N\}$  and  $x \in \{\omega_l, \psi_l, \varphi_{k,j}\}$ . The cascaded user-RIS-BS channel is

$$\mathbf{G}_k = \mathbf{H} \text{Diag}(\mathbf{h}_k) = \sum_{l=1}^L \sum_{j=1}^{J_k} \alpha_l \beta_{k,j} \mathbf{a}_N(\psi_l) \mathbf{a}_M^H(\omega_l - \varphi_{k,j}). \quad (16)$$

Existing papers estimated  $L$  AoAs,  $J_k L$  cascaded AoDs, and  $J_k L$  cascaded complex channel gains.

## Mult-user Case

$\mathbf{H}$  is reformulated as  $\mathbf{H} = \mathbf{A}_N \boldsymbol{\Lambda} \mathbf{A}_M^H$ , where  $\mathbf{A}_N = [\mathbf{a}_N(\psi_1), \dots, \mathbf{a}_N(\psi_L)]$ ,  $\boldsymbol{\Lambda} = \text{Diag}(\alpha_1, \alpha_2, \dots, \alpha_L)$  and  $\mathbf{A}_M = [\mathbf{a}_M(\omega_1), \dots, \mathbf{a}_M(\omega_L)]$ .

$\mathbf{h}_k$  is rewritten as  $\mathbf{h}_k = \mathbf{A}_{M,k} \boldsymbol{\beta}_k$ , where  $\boldsymbol{\beta}_k = [\beta_{k,1}, \dots, \beta_{k,J_k}]^T$  and  $\mathbf{A}_{M,k} = [\mathbf{a}_M(\varphi_{k,1}), \dots, \mathbf{a}_M(\varphi_{k,J_k})]$ .

Hence, the cascaded channel can be rewritten as

$$\mathbf{G}_k = \mathbf{A}_N \boldsymbol{\Lambda} \mathbf{A}_M^H \text{Diag}(\mathbf{A}_{M,k} \boldsymbol{\beta}_k), \forall k. \quad (17)$$

### Observations

- ① For each user, only  $J_k + L$  complex gains and  $2L + J_k$  angles that need to be estimated
- ② All users share the same  $L$  complex gains  $\{\alpha_l\}_{l=1}^L$  and  $2L$  angles  $\{\theta_l, \phi_l\}_{l=1}^L$

# Channel Estimation Protocol

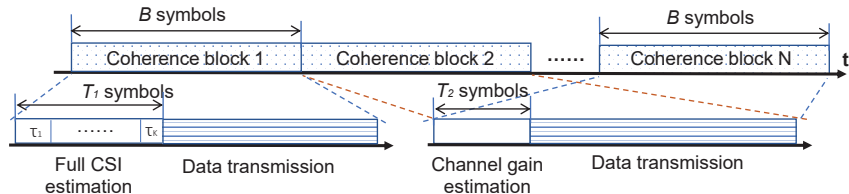


Figure 7: Channel estimation protocol and frame structure

## Key Concepts:

- ① Estimate the full CSI information at the first coherence block, including all the angle information and the channel gain
- ② Only need to estimate the channel gains in the remaining coherence blocks

# Channel Estimation Algorithm

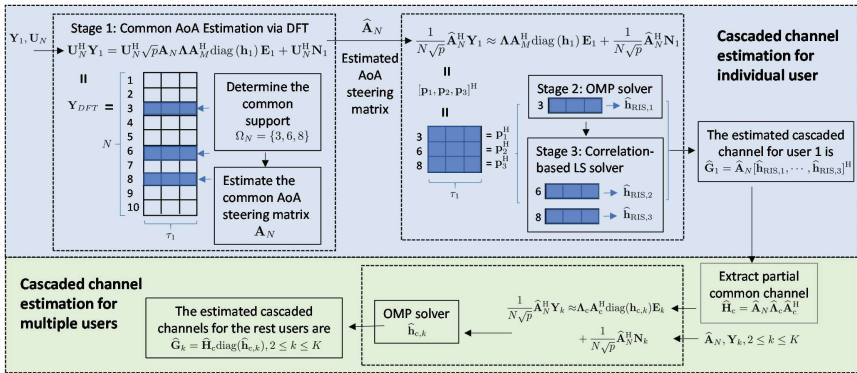


Figure 8: Cascaded channel estimation strategy for multiple users

# Simulation Results

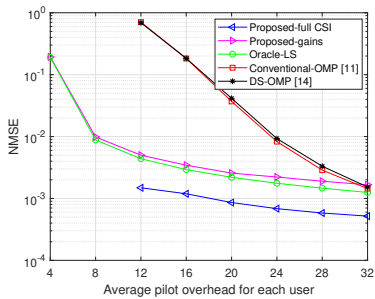


Figure 9: NMSE versus pilot overhead

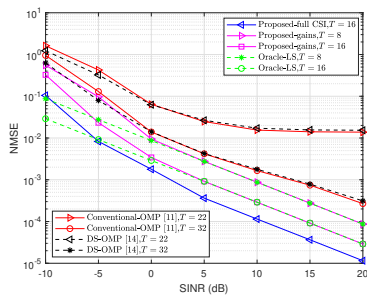


Figure 10: NMSE versus SNR

G. Zhou, C. Pan\*, H. Ren, P. Popovski and A. L. Swindlehurst, "Channel Estimation for RIS-Aided Multiuser Millimeter-Wave Systems," in IEEE Transactions on Signal Processing, vol. 70, pp. 1478-1492, 2022

# Error Propagation Reduced Scheme

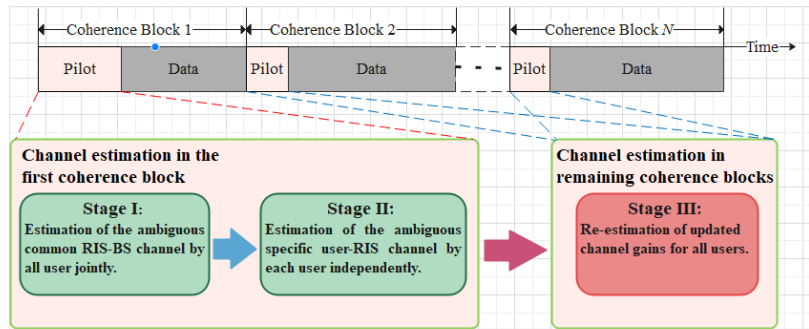


Figure 11: Error Propagation Reduced Scheme

# Error Propagation Reduced Scheme

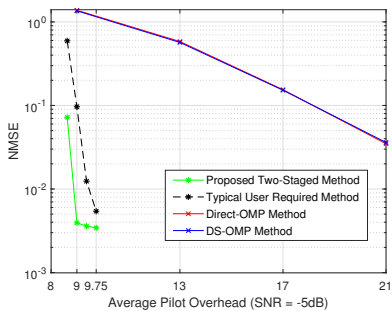


Figure 12: NMSEs vs. Average pilot overhead of each user

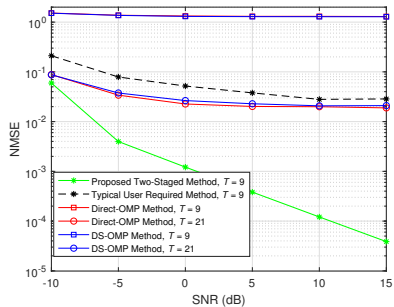


Figure 13: NMSEs vs. SNR for the ULA-type RIS case

Z. Peng, C. Pan\*, et al, "Channel Estimation for RIS-Aided Multi-User mmWave Systems with Reduced Error Propagation," to be submitted.

# Related References

- ① G. Zhou, C. Pan\*, H. Ren, P. Popovski and A. L. Swindlehurst, "Channel Estimation for RIS-Aided Multiuser Millimeter-Wave Systems," in IEEE Transactions on Signal Processing, vol. 70, pp. 1478-1492, 2022
- ② A. L. Swindlehurst, G. Zhou, R. Liu, C. Pan and M. Li, "Channel Estimation With Reconfigurable Intelligent Surfaces—A General Framework," in Proceedings of the IEEE, 2022
- ③ P. Wang, J. Fang, H. Duan, and H. Li, "Compressed channel estimation for intelligent reflecting surface-assisted millimeter wave systems," IEEE Signal Process. Lett., vol. 27, no. May, pp. 905 C909, 2020.
- ④ J. Chen, Y.-C. Liang, H. V. Cheng, and W. Yu, "Channel estimation for reconfigurable intelligent surface aided multi-user MIMO systems," 2019. [Online]. Available: <https://arxiv.org/abs/1912.03619>
- ⑤ K. Ardah, S. Gherekhloo, A. de Almeida, and M. Haardt, "TRICE: A channel estimation framework for RIS-aided millimeter-wave MIMO systems," IEEE Signal Process. Lett., vol. 28, pp. 513 C517, Feb. 2021.
- ⑥ T. Lin, X. Yu, Y. Zhu, and R. Schober, "Channel estimation for IRS- assisted millimeter-wave MIMO systems: Sparsity-inspired approach- es," IEEE Trans. Commun., vol. 70, no. 6, pp. 4078 C4092, 2022.
- ⑦ J. He, H. Wymeersch, and M. Juntti, "Channel estimation for RIS-aided mmWave MIMO systems via atomic norm minimization," IEEE Trans. Wireless Commun., vol. 20, no. 9, pp. 5786 C5797, Sept. 2021.
- ⑧ X. Wei, D. Shen, and L. Dai, "Channel estimation for RIS assisted wireless communications: Part II - an improved solution based on double-structured sparsity," IEEE Commun. Lett., vol. 25, no. 5, pp. 1403 C1407, May 2021.
- ⑨ Z. Peng, C. Pan\*, et al, "Channel Estimation for RIS-Aided Multi-User mmWave Systems with Reduced Error Propagation," to be submitted.

# Transmission Design

# Transmission Design in RIS Systems

How to jointly optimize the phase shifts  $\theta$  and beamforming vector  $\mathbf{w}$  to achieve the desired target remains a challenging problem.

## Rate Maximization

$$\max_{\mathbf{w}, \theta} R(\mathbf{w}, \theta) \quad (18a)$$

$$\text{s.t. } \|\mathbf{w}\|^2 \leq P_{\max}, \quad (18b)$$

$$|\theta_m|^2 = 1, \forall m, \quad (18c)$$

## Power Minimization

$$\min_{\mathbf{w}, \theta} \|\mathbf{w}\|^2 \quad (19a)$$

$$\text{s.t. } R(\mathbf{w}, \Phi) \geq R_{\min}, \quad (19b)$$

$$|\theta_m|^2 = 1, \forall m, \quad (19c)$$

where (18b) is power constraint, and (18c) is the unit-modulus constraint.

where (19b) is rate requirement, (19c) is the unit-modulus constraint.

# Two Transmission Protocols

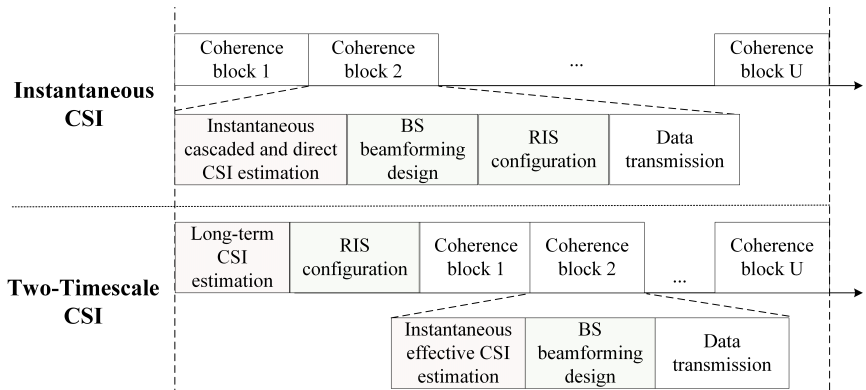


Figure 14: Transmission designs based on different levels of CSI availability.

Y. Han, W. Tang, S. Jin, C. -K. Wen and X. Ma, "Large Intelligent Surface-Assisted Wireless Communication Exploiting Statistical CSI," in IEEE Transactions on Vehicular Technology, vol. 68, no. 8, pp. 8238-8242, Aug. 2019

# Instantaneous CSI

# Instantaneous CSI

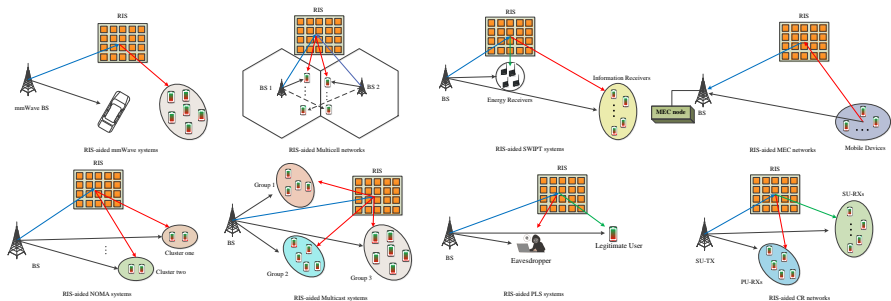


Figure 15: Typical applications of RIS in various emerging systems.

C. Pan et al., "Reconfigurable Intelligent Surfaces for 6G Systems: Principles, Applications, and Research Directions," in IEEE Communications Magazine, vol. 59, no. 6, pp. 14-20, June 2021

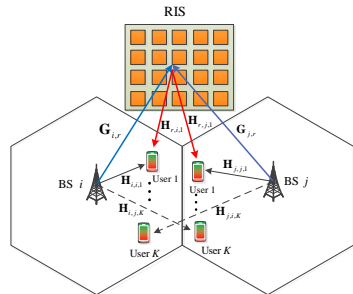
# RIS-aided Multicell MIMO Networks

## Challenges in Multicell Networks

- Weak signal power at the cell edge
- Cell-edge users suffer from severe inter-cell interference

## RIS-aided Multicell Networks

- Inter-cell interference can be alleviated
- Useful signal strength can be enhanced



**Design Objective:** Maximize the weighted sum-rate (WSR) of the system under two constraints:

- Each BS's individual power constraint
- Unit-modulus constraint of the RIS phase shifts

C. Pan, H. Ren, K. Wang, W. Xu, M. Elkashlan, A. Nallanathan, and L. Hanzo, "Multicell MIMO communications relying on intelligent reflecting surface", IEEE Transactions on Wireless Communications, vol. 19, no. 8, pp. 5218–5233, Aug. 2020.

# Complex Circle Manifold (CCM) Algorithm

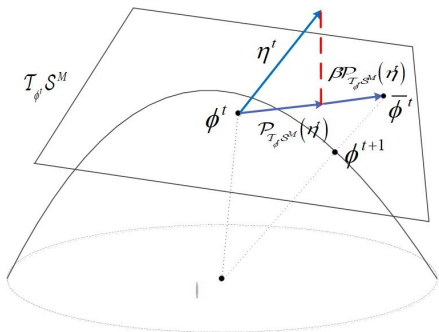


**Figure 16:** Geometric interpretation of the CCM algorithm.

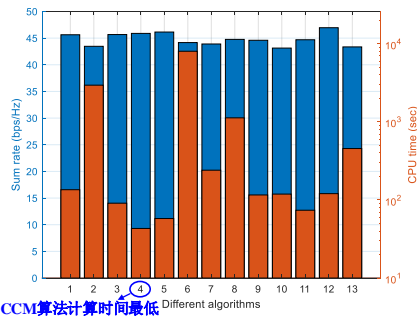


**Figure 17:** Sum rate and CPU time of different algorithms

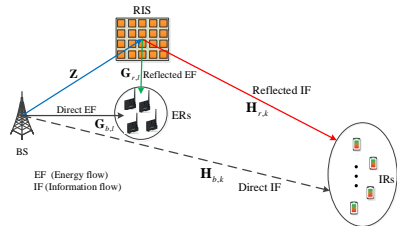
C. Pan, H. Ren, K. Wang, W. Xu, M. Elkashlan, A. Nallanathan, and L. Hanzo, "Multicell MIMO communications relying on intelligent reflecting surface", IEEE Transactions on Wireless Communications, vol. 19, no. 8, pp. 5218-5233, Aug. 2020.

C. Pan et al., "An Overview of Signal Processing Techniques for RIS/IRS-aided Wireless Systems," in IEEE Journal of Selected Topics in Signal Processing, 2022

# RIS-aided MIMO Broadcasting for SWIPT

**Hurdles in SWIPT:** Limited energy can be harvested due to severe signal attenuation

**RIS-aided SWIPT:** Enhance the harvested power at the energy receivers (ERs)



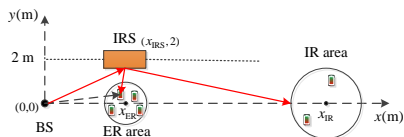
**Design Objective:** Maximize the WSR of the information receivers (IRs) under three constraints:

- BS's total power constraint
- Unit-modulus constraint of the IRS phase shifts
- Satisfy the energy harvesting requirement of the ERs

C. Pan, H. Ren, K. Wang, M. Elkashlan, J. Wang, and A. Nallanathan, L. Hanzo, "Intelligent Reflecting Surface Aided MIMO Broadcasting for Simultaneous Wireless Information and Power Transfer", IEEE Journal on Selected Areas in Communications, vol. 38, no. 8, pp. 1719-1734, Aug. 2020. (IEEE ComSoc Leonard G. Abraham Prize)

# RIS-aided MIMO Broadcasting for SWIPT

## Simulation Setup



- ① More energy can be harvested with the aid of IRS
- ② The amount of harvested energy increases rapidly with  $M$
- ③ Operational range of the ERs is extended with the aid of RIS

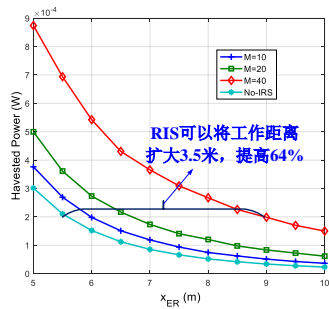


Figure 18: Maximum harvested power achieved by various schemes.

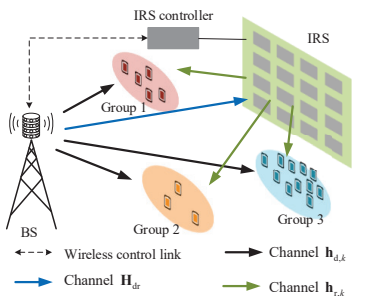
C. Pan, H. Ren, K. Wang, M. Elkashlan, J. Wang, and A. Nallanathan, "Intelligent Reflecting Surface Aided MIMO Broadcasting for Simultaneous Wireless Information and Power Transfer", IEEE Journal on Selected Areas in Communications, vol. 38, no. 8, pp. 1719-1734, Aug. 2020. (IEEE ComSoc Leonard G. Abraham Prize)

# IRS-aided Multigroup Multicast Communications

## Challenges in Multicast Comm.

- ① Date rate in each group is limited by the user with the worst channel condition
- ② Some users may be blocked or experience severe path loss

**IRS-aided Multicast Comm.:** Channel conditions for the worst-case user can be improved with the aid of IRS



**Design Objective:** Maximize the system capacity through jointly optimizing the active beamforming vectors and phase shift matrix subject to:

- Total power constraint at the BS
- Unit-modulus constraint of the IRS phase shifts

G. Zhou, C. Pan\*, H. Ren, K. Wang and A. Nallanathan, "Intelligent Reflecting Surface Aided Multigroup MISO Communication Systems," IEEE Transactions on Signal Processing, vol. 68, pp. 3236-3251, 2020.

# IRS-aided Multigroup Multicast Communications

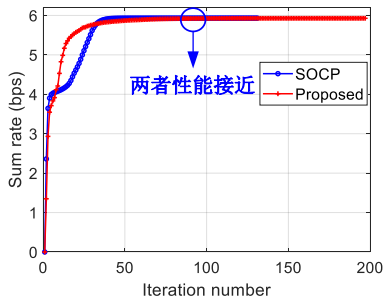


Figure 19: Sum rate performance of both algorithms.

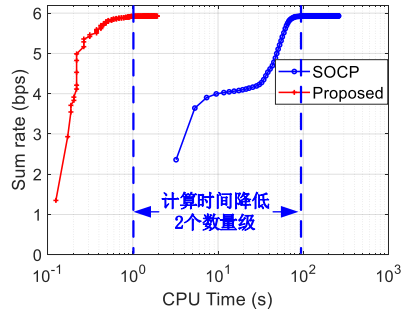


Figure 20: Running time of both algorithms.

G. Zhou, C. Pan\*, H. Ren, K. Wang and A. Nallanathan, "Intelligent Reflecting Surface Aided Multigroup Multicast MISO Communication Systems," IEEE Transactions on Signal Processing, vol. 68, pp. 3236-3251, 2020.

# Related References

- ① C. Pan et al., "Intelligent Reflecting Surface Aided MIMO Broadcasting for Simultaneous Wireless Information and Power Transfer," in IEEE Journal on Selected Areas in Communications, vol. 38, no. 8, pp. 1719-1734, Aug. 2020 (IEEE ComSoc Leonard G. Abraham Prize, ESI hot paper, ESI highly cited paper)
- ② C. Pan et al., "Multicell MIMO Communications Relying on Intelligent Reflecting Surfaces," in IEEE Transactions on Wireless Communications, vol. 19, no. 8, pp. 5218-5233, Aug. 2020. (ESI hot paper, ESI highly cited paper)
- ③ C. Pan et al., "Reconfigurable Intelligent Surfaces for 6G Systems: Principles, Applications, and Research Directions," in IEEE Communications Magazine, vol. 59, no. 6, pp. 14-20, June 2021 (ESI highly cited paper)
- ④ G. Zhou, C. Pan\*, H. Ren, K. Wang and A. Nallanathan, "Intelligent Reflecting Surface Aided Multigroup Multicast MISO Communication Systems," in IEEE Transactions on Signal Processing, vol. 68, pp. 3236-3251, 2020 (ESI highly cited paper)
- ⑤ T. Bai, C. Pan\*, Y. Deng, M. Elkashlan, A. Nallanathan and L. Hanzo, "Latency Minimization for Intelligent Reflecting Surface Aided Mobile Edge Computing," in IEEE Journal on Selected Areas in Communications, vol. 38, no. 11, pp. 2666-2682, Nov. 2020 (ESI highly cited paper)
- ⑥ S. Hong, C. Pan\*, H. Ren, K. Wang and A. Nallanathan, "Artificial-Noise-Aided Secure MIMO Wireless Communications via Intelligent Reflecting Surface," in IEEE Transactions on Communications, vol. 68, no. 12, pp. 7851-7866, Dec. 2020
- ⑦ Z. Peng, Z. Zhang, C. Pan, L. Li and A. L. Swindlehurst, "Multiuser Full-Duplex Two-Way Communications via Intelligent Reflecting Surface," in IEEE Transactions on Signal Processing, vol. 69, pp. 837-851, 2021
- ⑧ L. Zhang, Y. Wang, W. Tao, Z. Jia, T. Song and C. Pan, "Intelligent Reflecting Surface Aided MIMO Cognitive Radio Systems," in IEEE Transactions on Vehicular Technology, vol. 69, no. 10, pp. 11445-11457, Oct. 2020
- ⑨ T. Bai, C. Pan\*, H. Ren, Y. Deng, M. Elkashlan, and A. Nallanathan, "Resource allocation for intelligent reflecting surface aided wireless powered mobile edge computing in OFDM systems," IEEE Trans. Wireless Commun., vol. 20, no. 8, pp. 5389-5407, Aug. 2021.

# Robust Design based on Imperfect Instantaneous CSI

The cascaded channel model can be written as

$$\mathbf{G}_k = \widehat{\mathbf{G}}_k + \Delta \mathbf{G}_k, \forall k \in \mathcal{K}. \quad (20)$$

where  $\widehat{\mathbf{G}}_k$  is the estimated cascaded channel and  $\Delta \mathbf{G}_k$  is the corresponding channel error matrix.

Bounded CSI error model (BCEM): Statistical CSI error model (SCEM):

$$\mathcal{E}_k \triangleq \{\Delta \mathbf{G}_k \mid \|\Delta \mathbf{G}_k\|_F \leq \xi_{g,k}\} \quad \text{vec}(\Delta \mathbf{G}_k) \sim \mathcal{CN}(\mathbf{0}, \Sigma_{g,k}), \Sigma_{g,k} \succeq \mathbf{0}, \forall k$$

Problem Formulation:

$$\min_{\mathbf{F}, \mathbf{e}} \|\mathbf{F}\|_F^2 \quad (21a)$$

$$\text{s.t. } \mathcal{R}_k(\mathbf{F}, \mathbf{e}) \geq R_k, \forall \Delta \mathbf{G}_k \in \mathcal{E}_k,$$

$$|e_m|^2 = 1, 1 \leq m \leq M.$$

Problem Formulation:

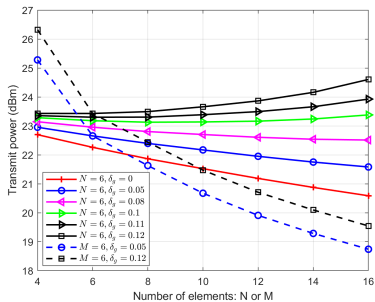
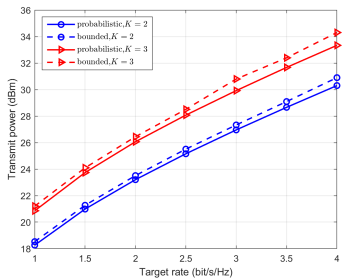
$$\min_{\mathbf{F}, \mathbf{e}} \|\mathbf{F}\|_F^2 \quad (22a)$$

$$\text{s.t. } \Pr\{\mathcal{R}_k(\mathbf{F}, \mathbf{e}) \leq R_k\} \leq \rho_k,$$

$$|e_m|^2 = 1, 1 \leq m \leq M.$$

G. Zhou, C. Pan\*, H. Ren, K. Wang and A. Nallanathan, "A Framework of Robust Transmission Design for IRS-Aided MISO Communications With Imperfect Cascaded Channels," IEEE Transactions on Signal Processing, vol. 68, pp. 5092-5106, 2020.

# Robust Design based on Imperfect Instantaneous CSI



- Worst-case robust design performs worse than the statistical one
- When channel uncertainty is small, the required power decreases with  $M$
- When channel uncertainty is large, the required power increases with  $M$

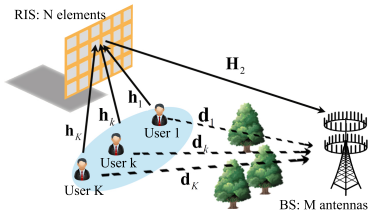
G. Zhou, C. Pan\*, H. Ren, K. Wang and A. Nallanathan, "A Framework of Robust Transmission Design for IRS-Aided MISO Communications With Imperfect Cascaded Channels," IEEE Transactions on Signal Processing, vol. 68, pp. 5092-5106, 2020.

# Related References

- ① G. Zhou, **C. Pan\***, H. Ren, K. Wang and A. Nallanathan, "A Framework of Robust Transmission Design for IRS-Aided MISO Communications With Imperfect Cascaded Channels," in IEEE Transactions on Signal Processing, vol. 68, pp. 5092-5106, 2020 ([ESI highly cited paper](#))
- ② S. Hong, **C. Pan\***, H. Ren, K. Wang, K. K. Chai and A. Nallanathan, "Robust Transmission Design for Intelligent Reflecting Surface-Aided Secure Communication Systems With Imperfect Cascaded CSI," in IEEE Transactions on Wireless Communications, vol. 20, no. 4, pp. 2487-2501, April 2021 ([ESI highly cited paper](#))
- ③ G. Zhou, **C. Pan\***, H. Ren, K. Wang, M. D. Renzo and A. Nallanathan, "Robust Beamforming Design for Intelligent Reflecting Surface Aided MISO Communication Systems," in IEEE Wireless Communications Letters, vol. 9, no. 10, pp. 1658-1662, Oct. 2020 ([ESI highly cited paper](#))
- ④ L. Zhang, **C. Pan\***, Y. Wang, H. Ren and K. Wang, "Robust Beamforming Design for Intelligent Reflecting Surface Aided Cognitive Radio Systems With Imperfect Cascaded CSI," in IEEE Transactions on Cognitive Communications and Networking, vol. 8, no. 1, pp. 186-201, March 2022
- ⑤ G. Zhou, **C. Pan\***, H. Ren, K. Wang, K. K. Chai and K. -K. Wong, "User cooperation for IRS-aided secure MIMO systems," in Intelligent and Converged Networks, vol. 3, no. 1, pp. 86-102, March 2022
- ⑥ Z. Peng, Z. Chen, **C. Pan\***, G. Zhou and H. Ren, "Robust Transmission Design for RIS-Aided Communications With Both Transceiver Hardware Impairments and Imperfect CSI," in IEEE Wireless Communications Letters, vol. 11, no. 3, pp. 528-532, March 2022

## Two-timescale CSI

# System Model



- $\alpha_k$ ,  $\beta$  and  $\gamma_k$ : large-scale fading coefficients
- $\varepsilon_k$  and  $\delta$ : Rician factors
- $\tilde{\mathbf{h}}_k^t$ ,  $\tilde{\mathbf{H}}_2^t$  and  $\tilde{\mathbf{d}}_k^t$ : NLoS channels
- $\bar{\mathbf{h}}_k$  and  $\bar{\mathbf{H}}_2$ : LoS channels
- $\Phi^t = \text{diag} \left\{ e^{j\theta_1^t}, \dots, e^{j\theta_N^t} \right\}$

In the  $t$ -th channel coherence time (CCT), CSI between user  $k$  and the RIS is

$$\mathbf{h}_k^t = \sqrt{\alpha_k} \left( \sqrt{\frac{\varepsilon_k}{\varepsilon_k + 1}} \bar{\mathbf{h}}_k + \sqrt{\frac{1}{\varepsilon_k + 1}} \tilde{\mathbf{h}}_k^t \right)$$

Channel between the RIS and the BS is

$$\mathbf{H}_2^t = \sqrt{\beta} \left( \sqrt{\frac{\delta}{\delta + 1}} \bar{\mathbf{H}}_2 + \sqrt{\frac{1}{\delta + 1}} \tilde{\mathbf{H}}_2^t \right)$$

Direct channel between user  $k$  and the BS is

$$\mathbf{d}_k^t = \sqrt{\gamma_k} \tilde{\mathbf{d}}_k^t$$

Overall channel between user  $k$  and the BS is

$$\mathbf{g}_k^t + \mathbf{d}_k^t = \mathbf{H}_2^t \Phi^t \mathbf{h}_k^t + \mathbf{d}_k^t$$

# Conventional Instantaneous CSI-Based Design

In the  $t$ -th CCT, with MRC receiver, the decoded signal for user  $k$  is given by

$$r_k^t = \sum_{i=1}^K \sqrt{p_i} (\mathbf{g}_k^t + \mathbf{d}_k^t)^H (\mathbf{g}_i^t + \mathbf{d}_i^t) x_i + (\mathbf{g}_k^t + \mathbf{d}_k^t)^H \mathbf{n}^t,$$

where  $\mathbf{g}_k^t = \mathbf{H}_2^t \Phi^t \mathbf{h}_k^t$ .

Denote by  $\mathbf{G}_k^t = \mathbf{H}_2^t \text{diag}(\mathbf{h}_k^t)$  and  $\mathbf{e}^t = [e^{j\theta_1^t}, \dots, e^{j\theta_N^t}]^T \in \mathbb{C}^{N \times 1}$ , the decoded signal for user  $k$  can be rewritten as

$$r_k^t = \sum_{i=1}^K \sqrt{p_i} (\mathbf{G}_k^t \mathbf{e}^t + \mathbf{d}_k^t)^H (\mathbf{G}_k^t \mathbf{e}^t + \mathbf{d}_i^t) x_i + (\mathbf{G}_k^t \mathbf{e}^t + \mathbf{d}_k^t)^H \mathbf{n}^t,$$

The SINR of user  $k$  is given by

$$\gamma_k^t = \frac{p_k \| \mathbf{G}_k^t \mathbf{e}^t + \mathbf{d}_k^t \|^4}{\sum_{i=1, i \neq k}^K p_i \left| (\mathbf{G}_k^t \mathbf{e}^t + \mathbf{d}_k^t)^H (\mathbf{G}_i^t \mathbf{e}^t + \mathbf{d}_i^t) \right|^2 + \sigma^2 \| \mathbf{G}_k^t \mathbf{e}^t + \mathbf{d}_k^t \|^2}$$

---

K. Zhi, C. Pan\*, H. Ren and K. Wang, "Power Scaling Law Analysis and Phase Shift Optimization of RIS-Aided Massive MIMO Systems With Statistical CSI," in IEEE Transactions on Communications, vol. 70, no. 5, pp. 3558-3574, May 2022

# Conventional Instantaneous CSI-Based Design

For each user  $k$ , one needs to estimate the cascaded channel  $\mathbf{G}_k^t$  and direct channel  $\mathbf{d}_k^t$ , the minimum number of time slots needed is

$$\tau \geq 2K + N - 1.$$

The date rate for each user  $k$  is

$$R_k^t = \left(1 - \frac{2K + N - 1}{\tau_c}\right) \log_2(1 + \gamma_k^t),$$

where  $\tau_c$  is the total number of time slots in each CCT.

**Max-min Problem:** Optimize the phase shifts for **each CCT** to maximize the minimum user date rate

$$\begin{aligned} & \max_{\Phi^t} \quad \min_k [R_k]^t \\ & \text{s.t. } \theta_n^t \in [0, 2\pi), \forall n \end{aligned}$$

GA method is used to solve this optimization problem.

---

K. Zhi, C. Pan\*, H. Ren and K. Wang, "Power Scaling Law Analysis and Phase Shift Optimization of RIS-Aided Massive MIMO Systems With Statistical CSI," in IEEE Transactions on Communications, vol. 70, no. 5, pp. 3558-3574, May 2022

## Two Time-scale Design

In the  $t$ -th CCT, with MRC receiver, the decoded signal for user  $k$  is given by

$$r_k^t = \sum_{i=1}^K \sqrt{p_i} (\mathbf{g}_k^t + \mathbf{d}_k^t)^H (\mathbf{g}_i^t + \mathbf{d}_i^t) x_i + (\mathbf{g}_k^t + \mathbf{d}_k^t)^H \mathbf{n}^t,$$

where  $\mathbf{g}_k^t = \mathbf{H}_2^t \Phi \mathbf{h}_k^t$ .

In the  $t$ -th CCT, the SINR of user  $k$  is given by

$$\gamma_k^t = \frac{p_k \|\mathbf{g}_k^t + \mathbf{d}_k^t\|^4}{\sum_{i=1, i \neq k}^K p_i \left| (\mathbf{g}_k^t + \mathbf{d}_k^t)^H (\mathbf{g}_i^t + \mathbf{d}_i^t) \right|^2 + \sigma^2 \|\mathbf{g}_k^t + \mathbf{d}_k^t\|^2}$$

To estimate overall channel  $\mathbf{g}_k^t + \mathbf{d}_k^t$ ,  $\forall k$ , the minimum number of time slots is

$$\tau = K$$

Then, the date rate for user  $k$  in the  $t$ -th CCT is

$$R_k^t = \left(1 - \frac{K}{\tau_c}\right) \log_2 (1 + \gamma_k^t).$$

# Two Time-scale Design

Over  $T$  CCT, the ergodic rate expression of user  $k$  is

$$R_k = \mathbb{E} \{ R_k^t \},$$

where the expectation is taken over the NLoS channel, e.g.,  $\tilde{\mathbf{h}}_k^t$ ,  $\tilde{\mathbf{H}}_2^t$  and  $\tilde{\mathbf{d}}_k^t$ .

The ergodic date rate of user  $k$  can be approximated as

$$R_k \approx \log_2 \left( 1 + \frac{p_k E_k^{(\text{signal})}(\Phi)}{\sum_{i=1, i \neq k}^K p_i I_{ki}(\Phi) + \sigma^2 E_k^{(\text{noise})}(\Phi)} \right),$$

where

$$E_k^{(\text{signal})}(\Phi) \triangleq \mathbb{E} \left\{ \| \mathbf{g}_k^t + \mathbf{d}_k^t \|^4 \right\},$$

$$I_{ki}(\Phi) \triangleq \mathbb{E} \left\{ \left| (\mathbf{g}_k^t + \mathbf{d}_k^t)^H (\mathbf{g}_i^t + \mathbf{d}_i^t) \right|^2 \right\},$$

$$E_k^{(\text{noise})}(\Phi) \triangleq \mathbb{E} \left\{ \| \mathbf{g}_k^t + \mathbf{d}_k^t \|^2 \right\}.$$

K. Zhi, C. Pan\*, H. Ren and K. Wang, "Power Scaling Law Analysis and Phase Shift Optimization of RIS-Aided Massive MIMO Systems With Statistical CSI," in IEEE Transactions on Communications, vol. 70, no. 5, pp. 3558-3574, May 2022

## Two Time-scale Design:

**Max-min Problem:** Optimize the phase shifts to maximize the minimum average data rate for each user:

$$\begin{aligned} \max_{\Phi} \quad & \min_k R_k \\ \text{s.t. } & \theta_n \in [0, 2\pi), \forall n \end{aligned}$$

Genetic algorithm (GA) method to solve the phase shift problem

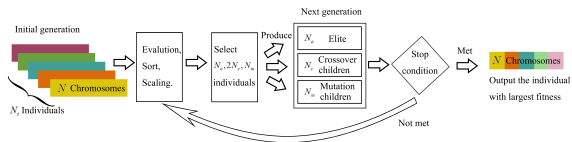


Figure 21: The diagram of GA-based method.

K. Zhi, C. Pan\*, H. Ren and K. Wang, "Power Scaling Law Analysis and Phase Shift Optimization of RIS-Aided Massive MIMO Systems With Statistical CSI," in IEEE Transactions on Communications, vol. 70, no. 5, pp. 3558-3574, May 2022

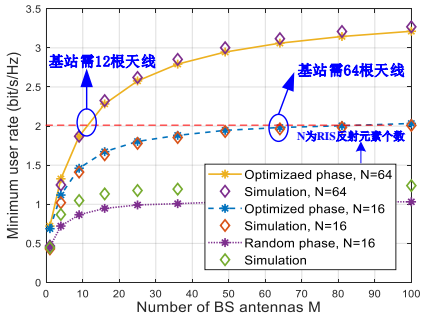
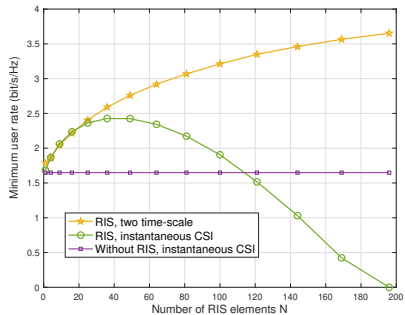
# Summary of Power Scaling Laws for Multiuser Case

Table 2: Power scaling laws under different channel conditions

		(RIS-BS channel, user-RIS channels)			
		(Rician, Rician)	(Rician, Rayleigh)	(Rayleigh, Rician)	(Rayleigh, Rayleigh)
Imperfect CSI	$M$	$1/M$	$1/M$	$1/\sqrt{M}$	$1/\sqrt{M}$
	$N$	\	$1/N$	$1/N$	$1/N$
Perfect CSI	$M$			$1/M$	
	$N$	\			$1/N$

K. Zhi, C. Pan\*, et al, "Two-Timescale Design for Reconfigurable Intelligent Surface-Aided Massive MIMO Systems with Imperfect CSI", major revision in IEEE Transactions on Information Theory, <https://arxiv.org/abs/2108.07622>

# Simulation Results



- ① Two time-scale scheme outperforms instantaneous CSI-based design
- ② The instantaneous CSI-based design firstly increases but then decreases
- ③ Power-hungry antennas at the BS can be replaced by low-power reflecting elements at the RIS

K. Zhi, C. Pan\*, H. Ren and K. Wang, "Power Scaling Law Analysis and Phase Shift Optimization of RIS-Aided Massive MIMO Systems With Statistical CSI," in IEEE Transactions on Communications, vol. 70, no. 5, pp. 3558-3574, May 2022

# Related References

- ① K. Zhi, **C. Pan\***, H. Ren and K. Wang, "Power Scaling Law Analysis and Phase Shift Optimization of RIS-Aided Massive MIMO Systems With Statistical CSI," in IEEE Transactions on Communications, vol. 70, no. 5, pp. 3558-3574, May 2022
- ② K. Zhi, **C. Pan\***, G. Zhou, H. Ren, M. Elkashlan and R. Schober, "Is RIS-Aided Massive MIMO Promising with ZF Detectors and Imperfect CSI?," in IEEE Journal on Selected Areas in Communications, 2022
- ③ K. Zhi, **C. Pan\***, et al, "Two-Timescale Design for Reconfigurable Intelligent Surface-Aided Massive MIMO Systems with Imperfect CSI", major revision in IEEE Transactions on Information Theory, <https://arxiv.org/abs/2108.07622>
- ④ K. Zhi, **C. Pan\***, H. Ren and K. Wang, "Ergodic Rate Analysis of Reconfigurable Intelligent Surface-Aided Massive MIMO Systems With ZF Detectors," in IEEE Communications Letters, vol. 26, no. 2, pp. 264-268, Feb. 2022
- ⑤ K. Zhi, **C. Pan\***, H. Ren and K. Wang, "Statistical CSI-Based Design for Reconfigurable Intelligent Surface-Aided Massive MIMO Systems With Direct Links," in IEEE Wireless Communications Letters, vol. 10, no. 5, pp. 1128-1132, May 2021
- ⑥ Z. Peng, T. Li, **C. Pan\***, H. Ren, W. Xu and M. D. Renzo, "Analysis and Optimization for RIS-Aided Multi-Pair Communications Relying on Statistical CSI," in IEEE Transactions on Vehicular Technology, vol. 70, no. 4, pp. 3897-3901, April 2021
- ⑦ Z. Peng, T. Li, **C. Pan\***, H. Ren and J. Wang, "RIS-Aided D2D Communications Relying on Statistical CSI With Imperfect Hardware," in IEEE Communications Letters, vol. 26, no. 2, pp. 473-477, Feb. 2022
- ⑧ Z. Peng, X. Chen, **C. Pan\***, M. Elkashlan and J. Wang, "Performance Analysis and Optimization for RIS-Assisted Multi-User Massive MIMO Systems with Imperfect Hardware," in IEEE Transactions on Vehicular Technology, 2022
- ⑨ Z. Peng, X. Liu, **C. Pan\***, L. Li and J. Wang, "Multi-Pair D2D Communications Aided by An Active RIS over Spatially Correlated Channels with Phase Noise," in IEEE Wireless Communications Letters, 2022
- ⑩ J. Dai, Y. Wang, **C. Pan\***, K. Zhi, H. Ren and K. Wang, "Reconfigurable Intelligent Surface Aided Massive MIMO Systems With Low-Resolution DACs," in IEEE Communications Letters, vol. 25, no. 9, pp. 3124-3128, Sept. 2021
- ⑪ J. Dai, F. Zhu, **C. Pan\***, H. Ren and K. Wang, "Statistical CSI-Based Transmission Design for Reconfigurable Intelligent Surface-Aided Massive MIMO Systems With Hardware Impairments," in IEEE Wireless Communications Letters, vol. 11, no. 1, pp. 38-42, Jan. 2022,
- ⑫ A. Papazafeiropoulos, **C. Pan**, P. Kourtessis, S. Chatzinotas and J. M. Senior, "Intelligent Reflecting Surface-Assisted MU-MISO Systems With Imperfect Hardware: Channel Estimation and Beamforming Design," in IEEE Transactions on Wireless Communications, vol. 21, no. 3, pp. 2077-2092, March 2022

# RIS-aided Localization/Sensing

# RIS-aided Localization/sensing

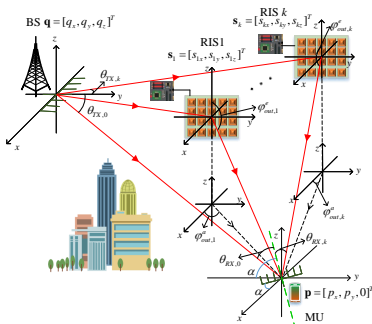


Figure 22: RIS-aided localization model.

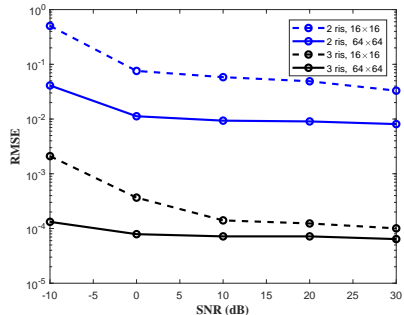


Figure 23: RMSE of the proposed algorithm versus SNR.

T. Wu, C. Pan\*, et al, "Two-Step mmWave Positioning Scheme with RIS-Part I: Angle Estimation and Analysis", submitted to IEEE Transactions on Signal Processing.

T. Wu, C. Pan\*, et al, "Two-Step mmWave Positioning Scheme with RIS-Part II: Position Estimation and Error Analysis", submitted to IEEE Transactions on Signal Processing.

# Near-field Channel

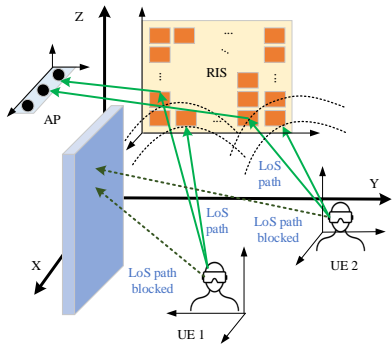


Figure 24: RIS-aided localization systems with near-field channels

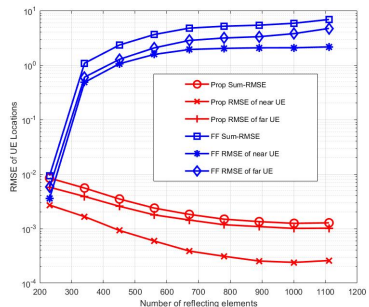


Figure 25: Positioning performance versus SNR

Y. Pan, C. Pan\*, et al. "Joint Channel Estimation and Localization in the Near Field of RIS Enabled mmWave/subTHz Communications", submitted to IEEE Transactions on Signal Processing

# Training Free Method

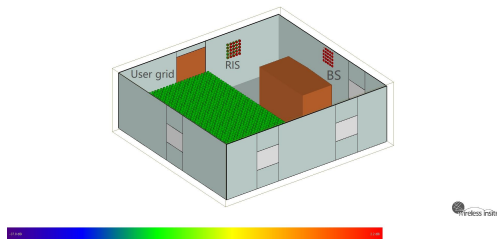


Figure 26: Simulated scenario

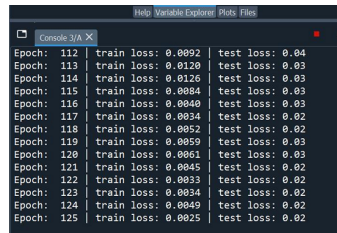


Figure 27: Simulated performance

---

T. Wu, C. Pan\*, et al, "RIS-aided Localization with Training Free Method", to be submitted.

# Future Research Directions

# Channel Tracking for Mobile Scenarios

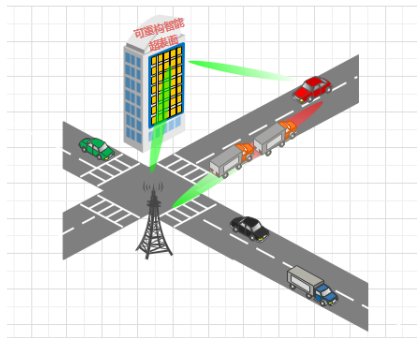


Figure 28: RIS-aided tracking system model

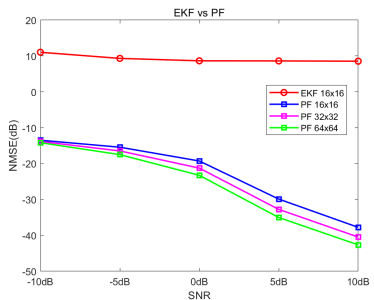


Figure 29: Tracking performance versus SNR

Y. Liu, M. Chen, **C. Pan\***, et al, "Channel Tracking for RIS-Assisted Wireless Communication Systems with Imperfect Cascaded Angle Information," , to be submitted.

# Active RIS

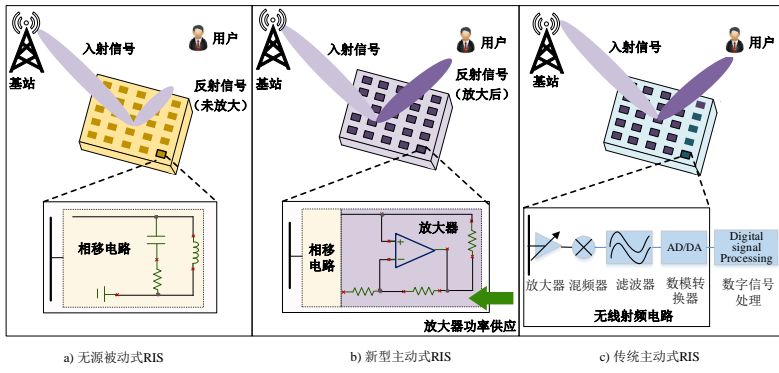


Figure 30: Circuit models of three kinds of RIS

Z. Zhang et al., "Active RIS vs. passive RIS: Which will prevail in 6G?" 2021, arXiv:2103.15154.

R. Long et al., "Active reconfigurable intelligent surface aided wireless communications," IEEE Trans. Wireless Commun., vol.

20, no. 8, pp. 4962-4975, Aug. 2021.

# Active RIS

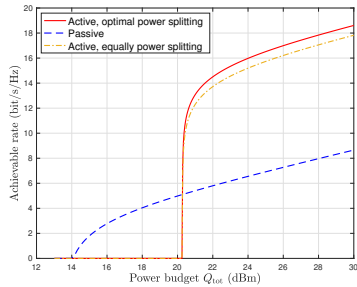


Figure 31: Rate comparison versus power budget

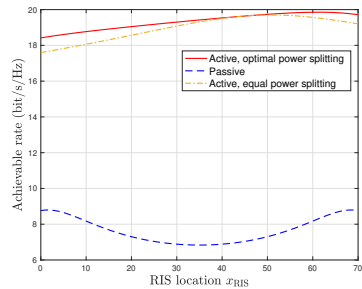


Figure 32: Rate comparison versus RIS location

K. Zhi, C. Pan\*, H. Ren, K. K. Chai and M. Elkashlan, "Active RIS Versus Passive RIS: Which is Superior With the Same Power Budget?," in IEEE Communications Letters, vol. 26, no. 5, pp. 1150-1154, May 2022

Z. Peng, X. Liu, C. Pan, L. Li and J. Wang, "Multi-Pair D2D Communications Aided by An Active RIS over Spatially Correlated Channels with Phase Noise," in IEEE Wireless Communications Letters, 2022

# STAR-RIS

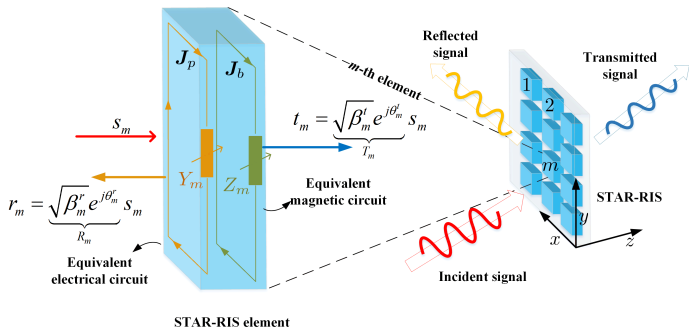


Figure 33: Schematic illustration of the STAR-RIS

J. Xu, Y. Liu, X. Mu and O. A. Dobre, "STAR-RISs: Simultaneous Transmitting and Reflecting Reconfigurable Intelligent Surfaces," in IEEE Communications Letters, vol. 25, no. 9, pp. 3134-3138, Sept. 2021

S. Zhang et al., "Intelligent Omni-Surfaces: Ubiquitous Wireless Transmission by Reflective-Refractive Metasurfaces," in IEEE Transactions on Wireless Communications, vol. 21, no. 1, pp. 219-233, Jan. 2022

# Double/multi-RIS

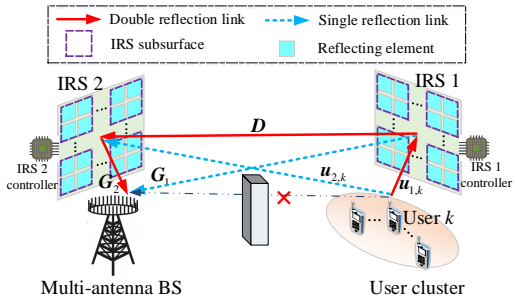


Figure 34: Double-RIS-aided communication systems

B. Zheng, C. You, and R. Zhang, "Double-IRS assisted multi-user MI- MO: Cooperative passive beamforming design," IEEE Trans. Wireless Commun., vol. 20, no. 7, pp. 4513 C4526, Jul. 2021.

Y. Han, S. Zhang, L. Duan, and R. Zhang, "Cooperative double-IRS aided communication: Beamforming design and power scaling," IEEE Wireless Commun. Letters, vol. 9, no. 8, pp. 1206 C1210, Aug. 2020.

H. Niu, Z. Chu, F. Zhou, **C. Pan**, D. W. K. Ng and H. X. Nguyen, "Double Intelligent Reflecting Surface-Assisted Multi-User MIMO Mmwave Systems With Hybrid Precoding," in IEEE Transactions on Vehicular Technology, vol. 71, no. 2, pp. 1575-1587, Feb. 2022

# Conclusions

- Cascaded CSI Estimation
  - For sub-6GHz frequency band, the pilot overhead is always **proportional to the number of reflecting elements** of RIS
  - For mmWave band, the pilot overhead can be reduced by exploiting the fact that all users share the **common BS-RIS channel**
- Transmission Design
  - For instantaneous CSI-based design, both perfect CSI and imperfect CSI are discussed
  - Two-timescale CSI-based method always performs better than the instantaneous CSI-based method when the number of reflecting elements is considered
- RIS-aided Localization/Sensing
  - ① The estimated angle error does not follow Gaussian distribution
  - ② Near-field channel model should be adopted
- Future research directions
  - ① Mobility tracking issue
  - ② Active RIS
  - ③ ...

# Thank you!

Email address: cpan@seu.edu.cn

Wechat ID: weiboPch007

Acknowledge my students and collaborators, including Gui Zhou, Kangda Zhi, Tuo Wu, Zhendong Peng, Zhangjie Peng, Shen Hong, Yijin Pan, Hong Ren, Jianxin Dai, Tong Bai, etc